CHAPTER-VII

NON-LINEAR OSCILLATIONS USING ANTISYMMETRIC TRANSFER CHARACTERISTICS OF A DIFFERENTIAL PAIR

7.1 INTRODUCTION

Oscillations in a regenerative circuit may be either in harmonic or relaxation mode, generating sinusoidal or non-sinusoidal waveforms respectively. The previous chapter has been devoted on a practical temperature and supply voltage insensitive sinewave oscillator using the self saturating characteristics of a transistor differential pair. The same circuit can be used to generate quasilinear and relaxation oscillations. Van der Pol[1] predicted that it is impracticable to obtain stable harmonic oscillation as well as relaxation oscillation from the same system as relaxation mode of operation is characterised by high degree of non-linearity and low order of selectivity and as such has requirement contrary to harmonic mode operation. Accordingly oscillators were partitioned into two distinct classes and treated separately. This precluded the possibility of having an unified analysis based on which the performance of a regenerative system could be predicted over the entire range from harmonic to relaxation mode and the parameters identified for adjustment for a particular mode of operation and wave form generation.

Adjustment from relaxation mode to stable harmonic mode of oscillation is, however, possible with a low-gain margin if proper modification is introduced with the optimized values of load and coupling elements together with the non-linearity of the antisymmetric transfer characteristic of a differential pair whereby the

output approaches the limiting value asymptotically. The non-linearity of the self-saturating characteristics is assumed to be a transcendental function of hyperbolic tangent type. An inverse tangent approximation of the amplifier function[2] was earlier proposed with limited success in predicting the practical oscillation waveform when operated at large amplitude. The anti-symmetric transfer characteristics introduces an instantaneous amplitude defining mechanism with reduced second harmonic distortion and makes the system self-compensating as regards parameter variation due to the change in ambient temperature and supply voltage variation[3], and much less critical for continuous control of operation from highly relaxed to harmonic mode. Realization of such an oscillator is interesting as it has a wide scope of control of its frequency and waveform making it useful as a test signal generator in various areas.

In this Chapter a comprehensive analytical approach to such a regenerative system with a particular type of non-linearity of the active circuit is presented[4*]. Through this approach its performance can be predicted over the entire range of operation and its operation can be controlled in a desired manner.

7.2 THE SYSTEM EQUATION

Instead of single parameter non-linear equation of van der Pol a more generalised equation of a non-linear oscillator has been derived here. This equation accounts more closely for the sharp rise and fall of the output voltage having a semi-exponential decay in between the relaxation, which cannot be obtained by the

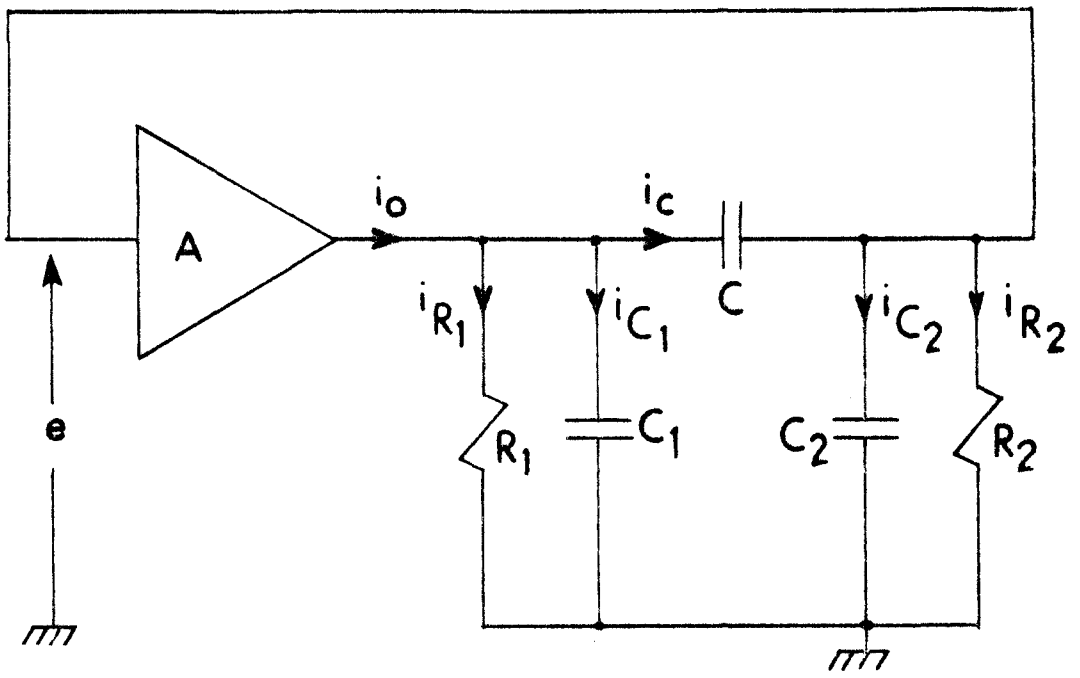

Fig. 7.1 Schematic of the oscillator

solution of the van der Pol equation in which the decay shows a convex nature. For a wide range of operation the non-linearity no longer remains restricted to a cubic function and probably this gives rise to the anomaly. It is now possible to suggest how the relative values of the two parameters may be changed to adjust the oscillation in a particular mode and generate a specific type of waveform.

Consider the oscillator shown in figure 7.1. The circuit equation is

$$\frac{1}{R_1}\left\{e + \frac{1}{C}\int\left(\frac{e}{R_2} + C_2\frac{de}{dt}\right)dt\right\} + C_1\left\{\frac{de}{dt} + \frac{1}{C}\left(\frac{e}{R_2} + C_2\frac{de}{dt}\right)\right\} + \frac{e}{R_2} + C_2\frac{de}{dt} = i_o \qquad (7.1)$$

Since the non-linearity of the self-saturating characteristic of the amplifier is utilized, the output current i_o will be a non-linear function of the input voltage e. Writing

$$i_o = a \tanh (be) \qquad (7.2)$$

as assumed and substituting equation (7.2) in equation (7.1) and differentiating equation (7.1) with respect to time and with the following substitutions :

(a) $R_2 = mR_1 = mR$

(b) $C_1 = n_1 C$

(c) $C_2 = n_2 C$

$$\left.\begin{aligned} &(d)\quad n = n_1 + n_2 + n_1 n_2 \\ &(e)\quad G = \frac{1}{mR}\,(1 + m + n_1 + mn_2) \\ &(f)\quad \omega_o^2 = \frac{1}{mnC^2R^2} \end{aligned}\right\} \qquad (7.3)$$

equation (7.1) reduces to

$$\frac{1}{\omega_o^2}\,\frac{d^2e}{dt^2} + (G - ab\ \mathrm{sech}^2 be)\,\frac{1}{\omega_o^2\, nC}\,\frac{de}{dt} + e = 0 \qquad (7.4)$$

Using the normalized parameter $\tau = \omega_o t$ equation (7.4) changes to

$$\frac{d^2e}{d\tau^2} - (ab - G)\,R\sqrt{\frac{m}{n}}\,\left(1 - \frac{ab}{ab - G}\,\tanh^2 be\right)\frac{de}{d\tau} + e = 0 \qquad (7.5)$$

The two parameters ϵ and β are defined as

$$\epsilon = (ab - G)\,R\sqrt{\frac{m}{n}} \qquad (7.6a)$$

$$\beta = \frac{ab}{ab - G} \qquad (7.6b)$$

Normalizing the parameter $e = \frac{V}{b}$, equation (7.5) now leads to the generalized expression of the non-linear differential equation for the regenerative system as

$$\frac{d^2V}{d\tau^2} - \epsilon\,(1 - \beta \tanh^2 V)\,\frac{dV}{d\tau} + V = 0 \qquad (7.7)$$

Since equation (7.7) is a trancendental equation, a closed form solution is not possible, except for the sinusoidal case when

$\epsilon = 0$. The numerical solution of the equation for non-sinusoidal wave is obtained with the help of a computer for different values of ϵ and β.

7.3 LIMITS OF PARAMETER VALUES

The parameters involved in constituting ϵ and β are R, m, n, G and ab, of which R, m, n and G are obtained from the passive parameter values and the factor ab is the slope of the normalized non-linear self-saturating transfer characteristics at the origin. Any values of the above parameters are not permissible and therefore it is necessary to set the limits of ϵ and β values. It can be seen from the following sections that ϵ and β cannot take-up any arbitrary value but must bear a relationship amongst themselves.

7.3.1 RATIO OF THE RESISTANCE m

Ideally $0 < m < \infty$, but for least component spread and brevity, m is assumed unity. Hence from equation (7.3a)

$$R_1 = R_2 = R \qquad (7.8)$$

7.3.2 RATIO OF THE CAPACITORS n_1 and n_2

Parameters n_1 and n_2 may have any positive value. It is evident from equation (7.3d) that n will have different values for various choices of n_1 and n_2.

It can be easily shown that

$$n_{max} = n_1 (2 + n_1) \text{ when } n_1 = n_2 \qquad (7.9a)$$

and

$$\left.\begin{aligned} n_{min} &= n_1 \quad \text{when } n_2 = 0 \\ &= n_2 \quad \text{when } n_1 = 0 \end{aligned}\right\} \qquad (7.9b)$$

Rigorous analysis do not permit either n_1 or n_2 to take up a zero value as C_1 or C_2 can never be zero, because even if lumped capacitors are absent the output, input and stray capacitances will contribute to C_1 and C_2, even though n_1 and n_2 may be very small.

For simplicity n_2 has been assumed zero whenever necessary and a finite positive value has been assigned to n_1. This could also be reversed without affecting the results so long as m is assumed unity [cf. equations (7.3d) and (7.3e)].

7.3.3 THE CIRCUIT CONDUCTANCE G

From equations (7.3e) and (7.8)

The parameter G is defined as

$$G = \frac{1}{R}(2 + n_1 + n_2) \qquad (7.10a)$$

or

$$n_1 + n_2 = GR - 2 \qquad (7.10b)$$

Thus for $n_1 + n_2$ = constant, G can have only one value larger than $\frac{2}{R}$ as $n_1 + n_2 > 0$.

For $n_1 + n_2$ = constant, m = 1, conductance parameter G is also held constant. Accordingly the limits for β and ϵ are evaluated holding this constant.

7.3.4 THE PARAMETER β

From equation (7.6a)

$$\beta = \frac{ab}{ab - G} \tag{7.11}$$

where ab is the slope of the antisymmetric self-saturating characteristics at the origin, this is constant for a particular operating condition.

Under the assumed conditions it has been shown that G can have only one value, hence β will also have only one value.

7.3.5 THE PARAMETER ϵ

From equations (7.6a) and (7.8)

$$\epsilon = (ab - G)\, R\sqrt{\frac{1}{n}} \tag{7.12}$$

Under the assumed conditions the value of ϵ will only vary with n and lie within a range ϵ_{max} and ϵ_{min} dependent upon n_{min} and n_{max} respectively. Combining equations (7.11) and (7.12) the maximum and minimum values of ϵ are given by

$$\epsilon_{max} = \frac{abR}{\beta}\sqrt{\frac{1}{n_{min}}} \tag{7.13a}$$

$$\epsilon_{min} = \frac{abR}{\beta}\sqrt{\frac{1}{n_{max}}} \tag{7.13b}$$

From the expression of ϵ it is seen that there is another constraint on the value of G. The value of G cannot be more than ab, in which case ϵ would be negative.

The parameters ϵ and β are quite interlinked. However, the effect of increasing ϵ is to increase distortion or harmonic contents of the wave and the effect of increase in β has a more pronounced effect on amplitude. This is well corroborated by computer solution.

7.3.6 EFFECT OF CONTROL OF ϵ and/or β

Since a two-parameter equation has been derived for the oscillator system, it may be of interest to note the effect of

(a) Changing ϵ keeping β constant,

(b) Changing β keeping ϵ constant,

and the conditions that are required to be met for such cases.

The first case has already been covered in subsection 7.3.5.

For the second case, from equation (7.13) one may write

$$\beta\sqrt{n} = \frac{K}{\epsilon} = \text{constant}, \text{ where } K = abR \qquad (7.14)$$

Since both β and n are dependent on n_1 and n_2 the range of values of these two quantities are to be found for which the product $\epsilon\beta\sqrt{n}$ will remain constant and equal to K. From equations (7.10) and (7.11)

$$\beta = \frac{abR}{(abR - 2)(n_1 + n_2)} \qquad (7.15)$$

The maximum and minimum values of β are therefore obtained by varying n_1 and n_2 as

$$\beta_{max} = \frac{abR}{(abR - 2) - n_1} \qquad \text{when } n_2 = 0 \tag{7.16}$$

and

$$\beta_{min} = \frac{abR}{(abR - 2) - 2n_1} \qquad \text{when } n_1 = n_2 \tag{7.17}$$

Obviously n_1 in equations (7.16) and (7.17) is not the same. Its values for the two cases can be evaluated from equations (7.14) and (7.15) involving ϵ besides a, b and R. Correspondingly β_{max} and β_{min} are then obtained as

$$\beta_{max} = \frac{abR}{(abR - 2) - \frac{\{2(abR-2) + \epsilon^2\} \pm \sqrt{4(abR-2)\epsilon^2 + \epsilon^4}}{2}} \tag{7.18}$$

$$\beta_{min} = \frac{abR}{(abR - 2) - 2\left[\frac{\{2(abR-2)+\epsilon^2\} \pm \sqrt{4(abR-2)\epsilon^2+\epsilon^4+\epsilon^2(abR-2)^2}}{4 - \epsilon^2}\right]} \tag{7.19}$$

7.4 THE SOLUTION OF THE DIFFERENTIAL EQUATION

The computerized solution of the differential equation [equation (7.7)] is based upon the modified Runge-Kutta method of numerical solution and its flow chart is given in figure 7.2.

7.5 COMPUTERIZED SOLUTION AND EXPERIMENTAL RESULTS

Three sets of computerized solutions and experimental results for verification were obtained for

(a) near sinusoidal oscillation
(b) near relaxation oscillation
(c) hard relaxation oscillation.

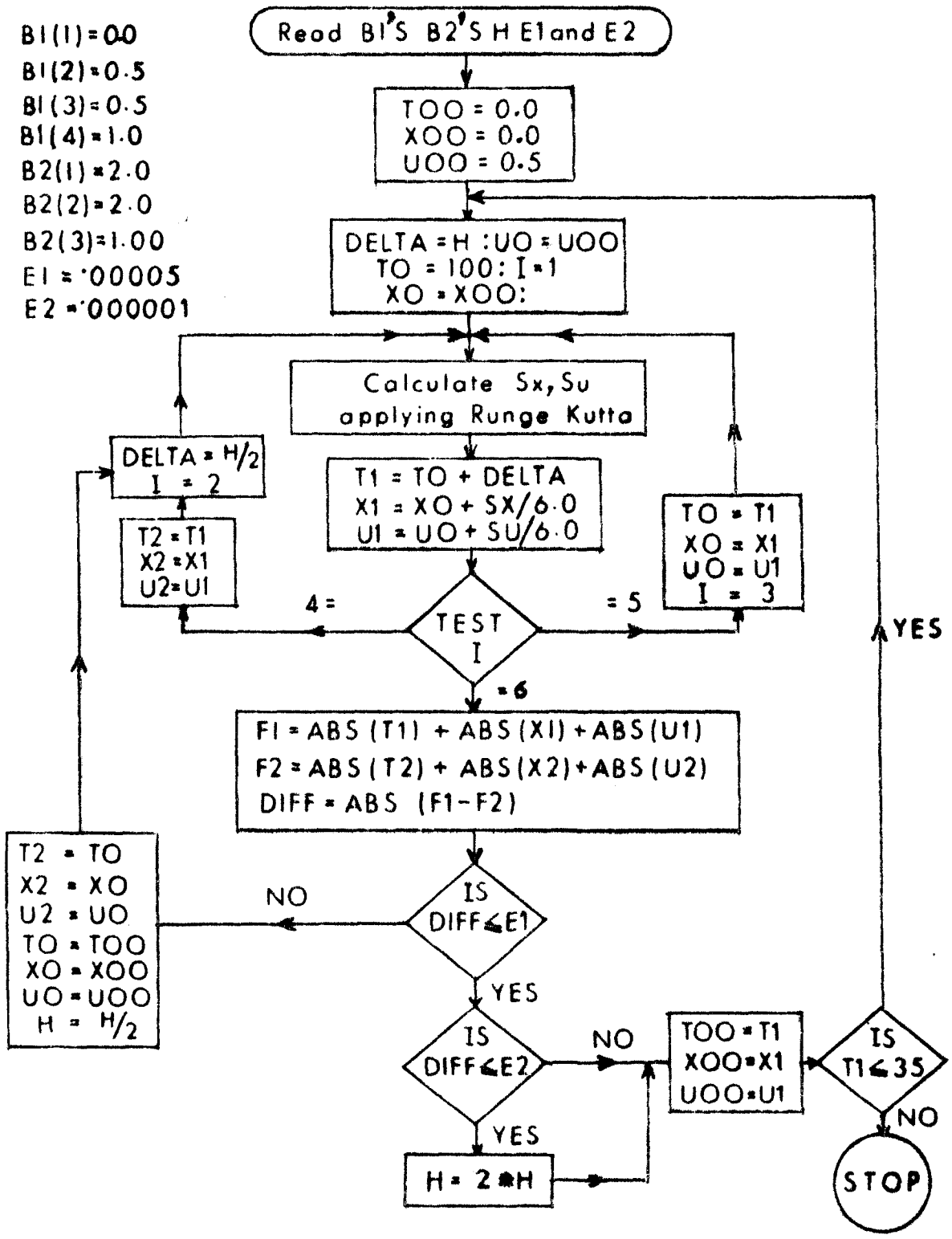

Fig.7.2. The programme flow chart. T and X in the chart correspond to τ and V in the text.

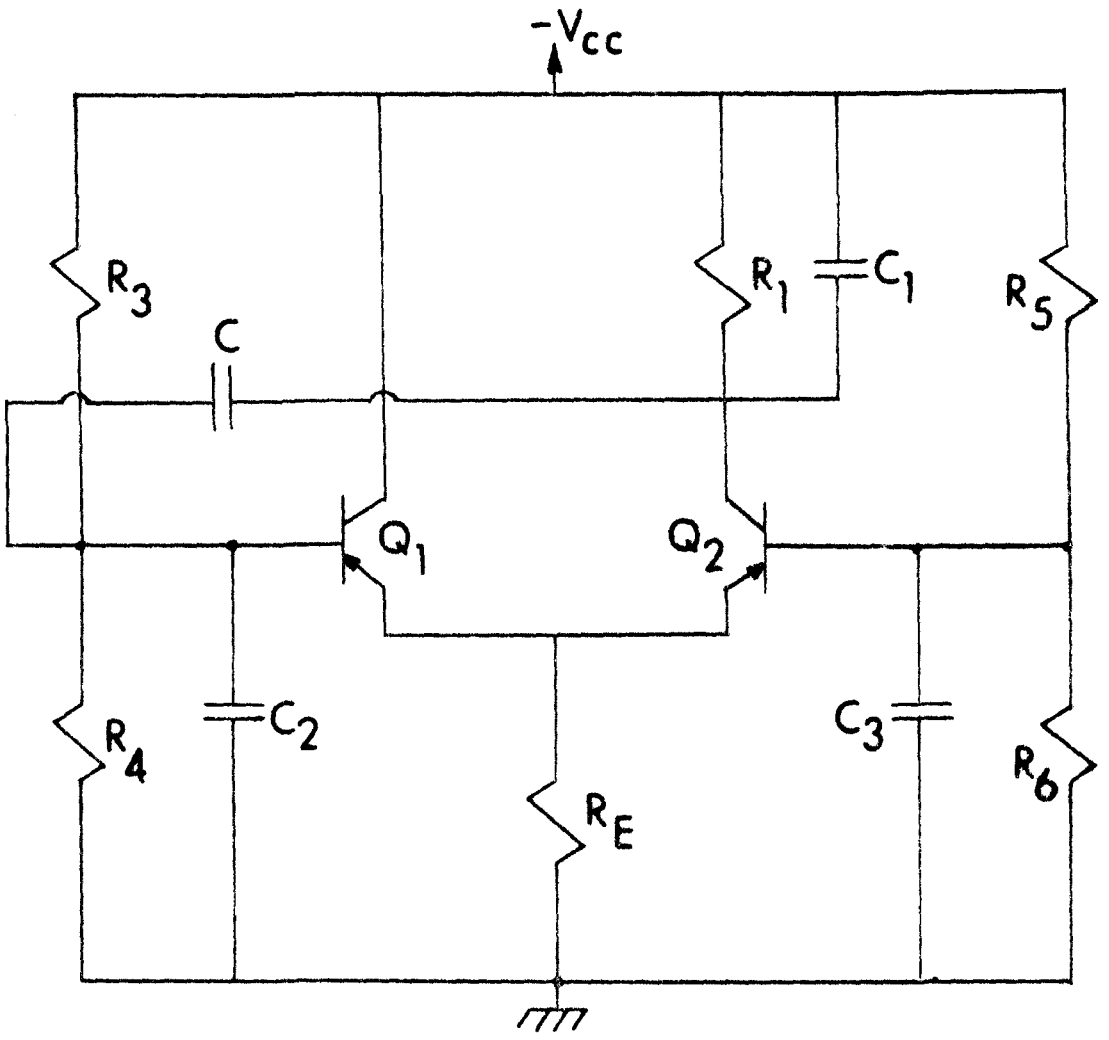

Fig. 7.3. The experimental circuit .

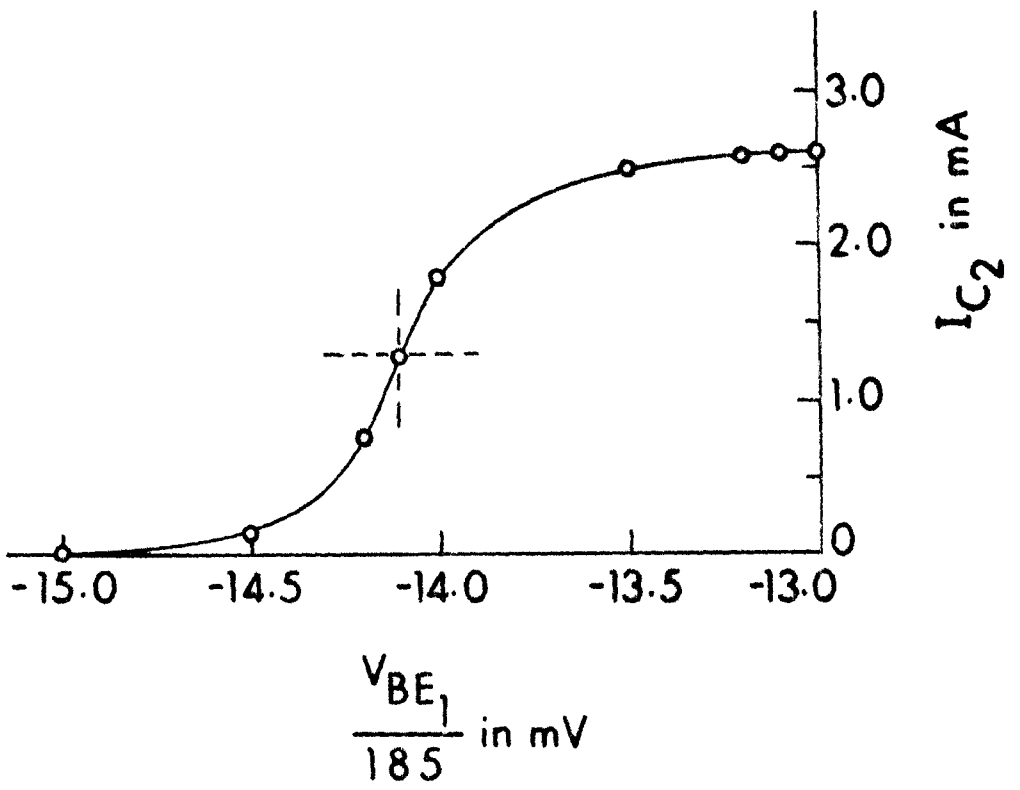

Fig.7.4. The antisymmetric self-saturating transfer characteristics of the differential pair.

The experimental circuit, as shown in figure 7.3 was initially adjusted for obtaining the slope ab, of the antisymmetric self-saturating characteristic of the differential pair shown in figure 7.4.

The different types of oscillation were obtained by changing the ratios of the capacitors i.e. n_1 and n_2 only, and the following parameters were kept constant at the denoted values for all the three cases.

R_1 = 1.35k ohms; m = 1; C = 0.011 μF and ab = 27.02 x 10^{-3} mhos.

TABLE-7.1

CONTROLLED PARAMETER AND DERIVED PARAMETER VALUES

Nature of Oscillation	Controlled Parameters		Derived Parameters			
	n_1	n_2	n	G	β	ϵ
Near Sinusoidal	10	10	120	16.30×10^{-3}	2.520	1.327
Near Relaxation	10	0.03	10	8.90×10^{-3}	1.490	7.740
Hard Relaxation	0.1	0.118	0.23	1.63×10^{-3}	1.069	74.600

Table-7.1 gives the controlled parameter and derived parameter values and Table-7.2 compares the calculated and experimental values of the frequency and amplitude of oscillation for the three cases.

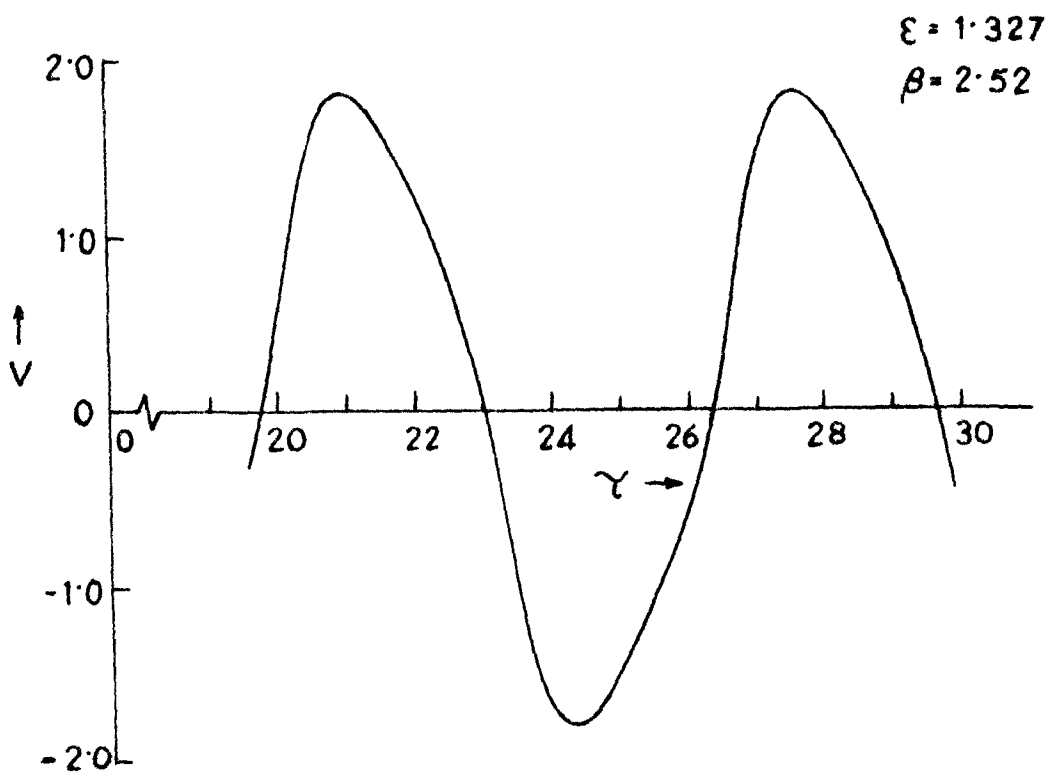

(a)

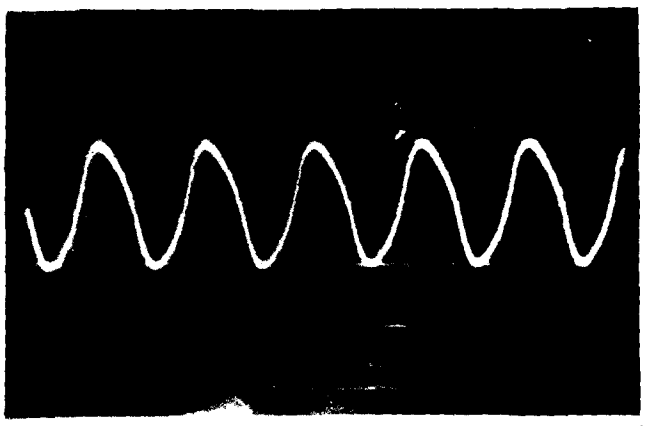

(b)

Fig.7.5. Waveforms for near sinusoidal oscillation. (a) Theoretical: (b) experimental: amplitude scale 100 mV per division.

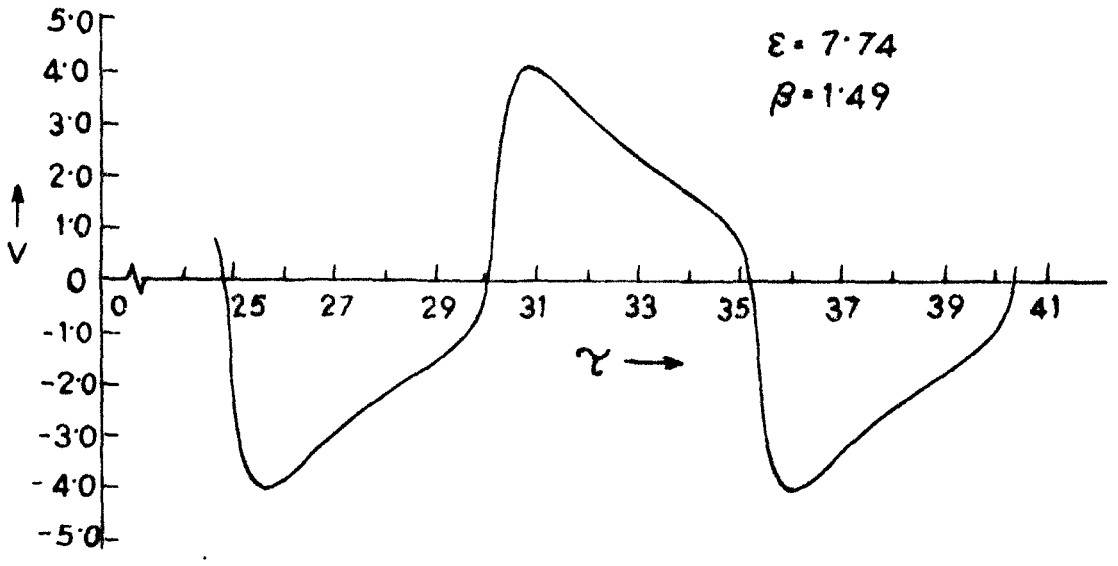

(a)

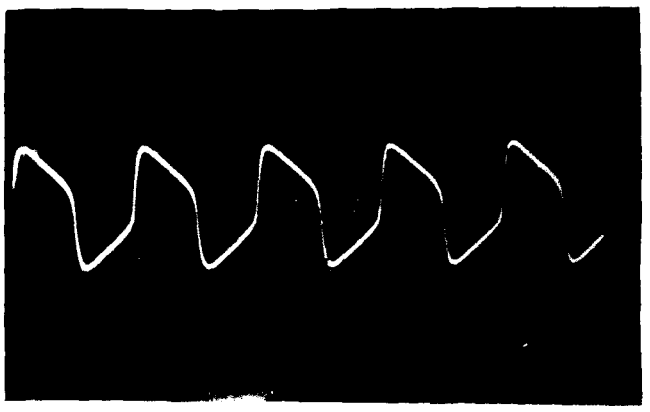

(b)

Fig. 7.6. Waveforms for near relaxation oscillation. (a) Theoretical: (b) experimental: amplitude scale 200 mV per division.

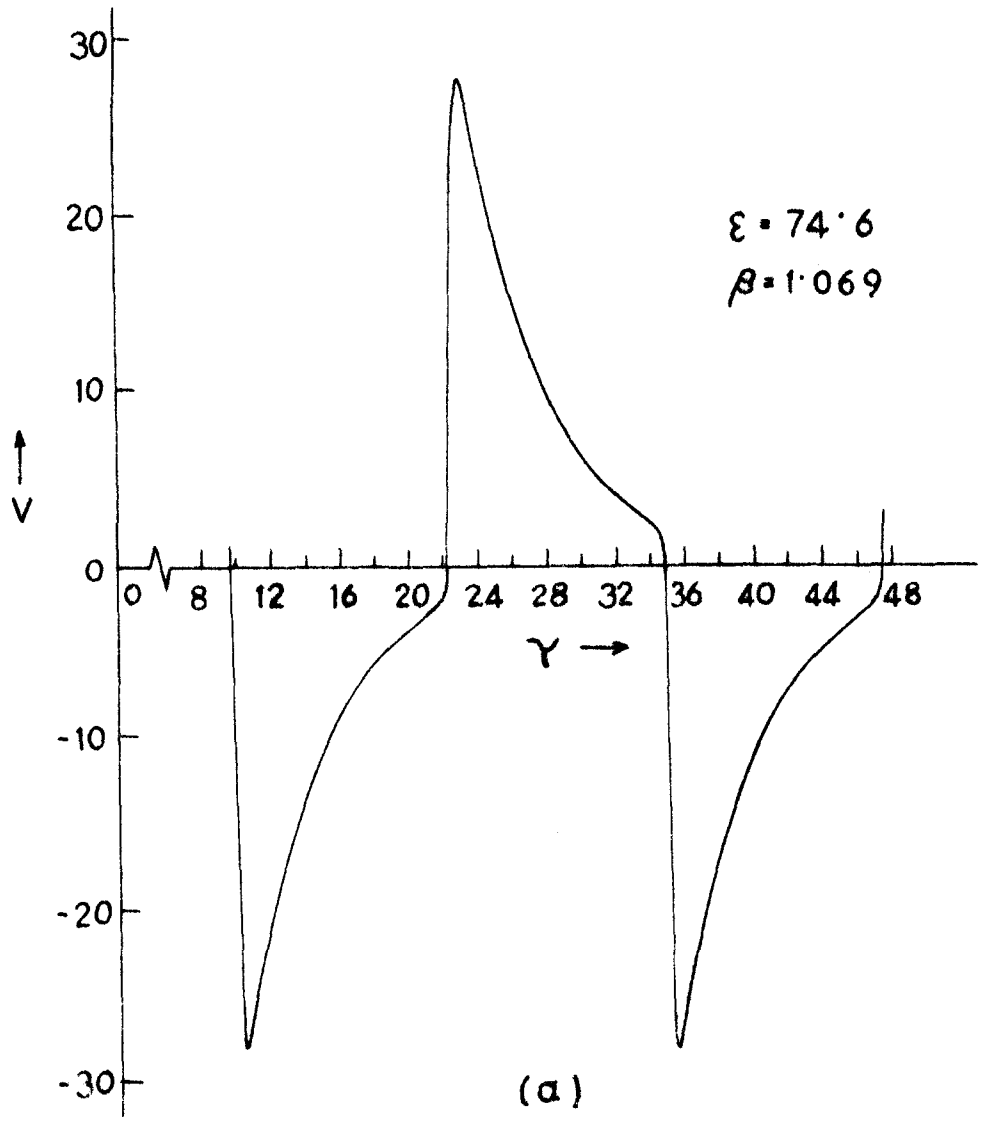

(a)

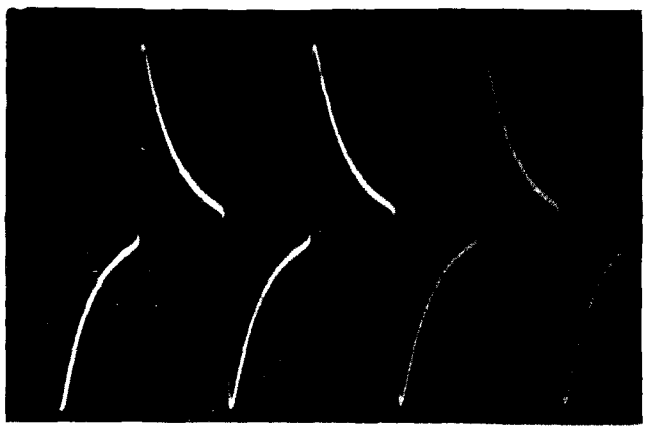

(b)

Fig.7.7. Waveforms for hard relaxation oscillation. (a) Theoretical; (b) experimental; amplitude scale 500 mV per division.

TABLE-7.2

CALCULATED AND EXPERIMENTAL VALUES OF FREQUENCY AND AMPLITUDE OF OSCILLATIONS

Nature of Oscillation	Amplitude of Oscillation Volts(Peak)		Frequency of Oscillation kHz	
	Calculated	Experimental	Calculated	Experimental*
Near Sinusoidal	0.087	0.095	0.935	0.980
Near Relaxation	0.197	0.200	2.050	2.150
Hard Relaxation	1.340	1.500	5.850	5.850

* Frequencies were measured with a counter

Though the assumed non-linearity gives a transcendental equation and a closed-form solution of equation (7.7) is not possible, from the results of Table-7.2, it is evident that the experimental results and theoretical numerical solution agree very well in all modes of oscillation, which is not so if the non-linearity is assumed to be of lesser complexity.

Figures 7.5(a), 7.5(b), 7.6(a), 7.6(b) and 7.7(a), 7.7(b) show the theoretical and experimental wave shapes for the three cases.

7.6 EFFECTS OF ϵ AND β ON DISTORTION AND AMPLITUDE

It has been stated that the effect of the parameter β has a predominant effect on amplitude and ϵ on distortion and this has been demonstrated in the curve of figures 7.8 and 7.9. Figures 7.8(a), 7.8(b) and 7.8(c) are plotted for constant β (β= 8.14)

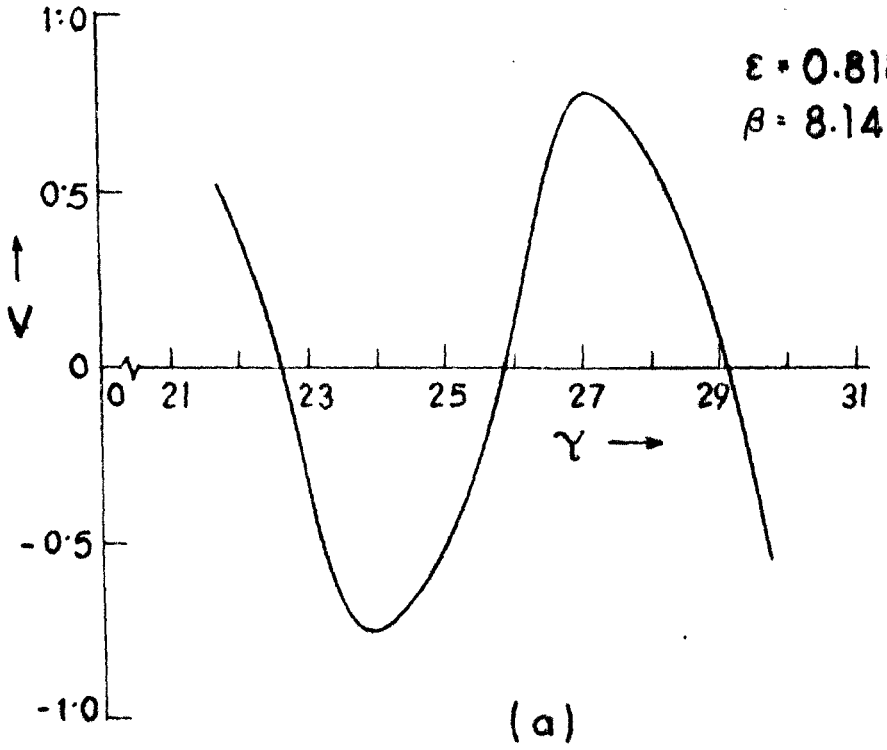

(a)

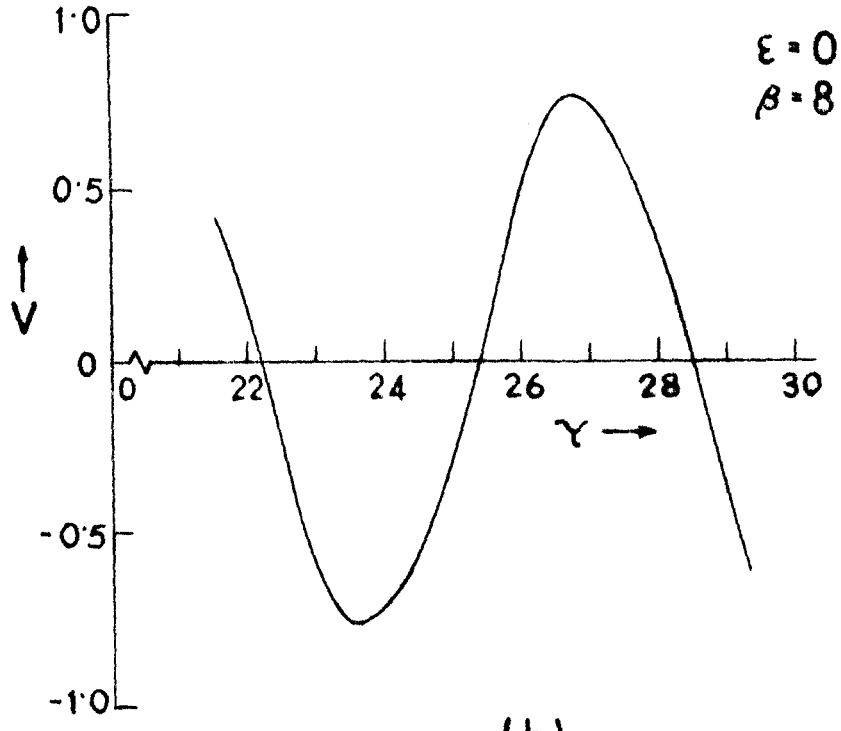

(b)

(continued over)

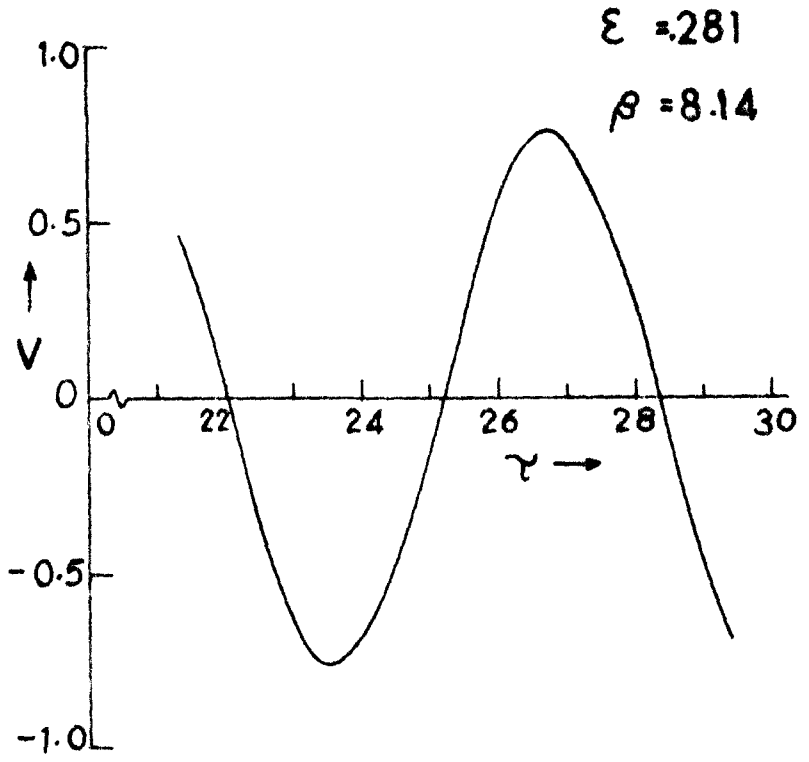

(c)

Fig. 7.8. Waveforms obtained for constant β (β = 8.14) and varying: (a) ϵ = 0.818; (b) ϵ = 0.485; (c) ϵ = 0.281.

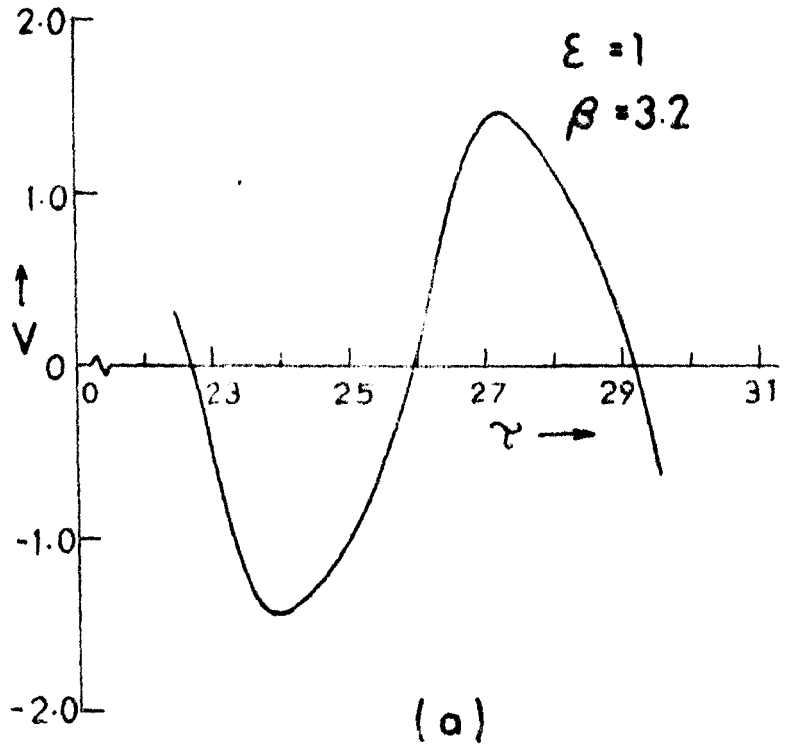

(a)

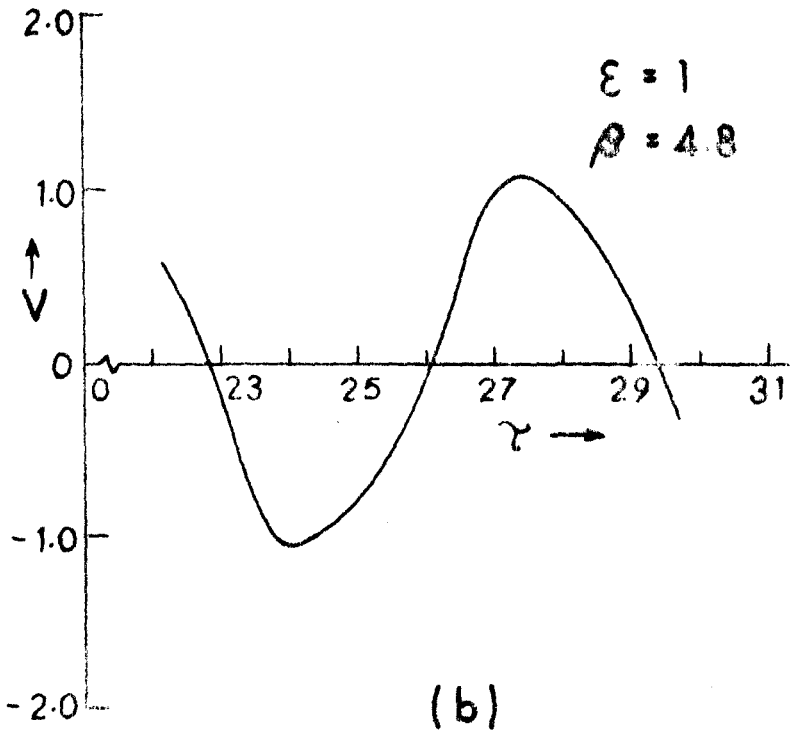

(b)

Fig. 7.9. Waveforms obtained for constant ϵ ($\epsilon = 1$) and varying: (a) $\beta = 3.2$: (b) $\beta = 4.8$.

and varying ϵ whose possible limits of variation are $0.818 \rangle \epsilon \rangle 0.281$. From the curves it is observed that the amplitude remains constant but the distortion increases slightly with increasing values of ϵ.

The next set of curves are plotted for constant ϵ ($\epsilon = 1$) and varying β over the possible limits $6.76 \rangle \beta \rangle 3.007$. Computerized solutions were obtained for $\epsilon = 1$ and $\beta = 3.2$ and $\beta = 4.8$ and have been plotted in figures 7.9(a) and 7.9(b). It is observed that the amplitude decreases with increase in the value of β.

7.7 THE VOLTAGE CONTROLLED OSCILLATOR[5*]

It has been shown so far, that oscillations in the system described may be controlled over harmonic to relaxation mode by controlling a passive parameter G obtained from the load and coupling elements. If G is held constant the mode of operation can still be controlled by varying the slope ab (at the origin) of the transfer characteristics. This slope can be varied quite simply by changing the operating bias voltage of one of the transistors of the differential pair and keeping that of the other constant. This in effect change the symmetric operation of the pair to asymmetric operation and the change in the average slope varies the parameter ϵ in equation (7.6a). This is effectively a voltage controlled oscillator (VCO) whose operation is gradually changed from harmonic mode to quasiharmonic mode, thereby changing the oscillation frequency due to harmonic depression[6]. However for a large frequency deviation, the distortion level still remains quite low and realization of a practical VCO is therefore envisaged.

The relation between the slope and the differential change in the bias voltage has been derived from the transfer characteristics [equation (7.2)] where e now represents the differential change in voltage and is replaced by u in subsequent discussion for clarity. Using this, a computerised solution of equation (7.7) is performed to obtain the frequency of VCO. The frequencies are also measured. The results are presented in Table-7.3 along with the results obtained by using the method of small parameters[6].

TABLE-7.3

RESULTS

[C = 1050pF, R = 2K, R_3 = 3.78K, R_4 = 2K, n = 9.476, m = 0.654, G = 8.509×10^{-3}mho, R_5 = 25Ω, h_{fe} = 500, I_{EE}=0.77mA; Ref.Fig.7.10(a)].

milli Volts	milli Siemen	Normalized frequency f/f_o^*			Measured distortion dB
		Computer Solution	Method of small parameter	Experimental	
1.78	10.240	0.9683	0.9483	0.9691	30
7.80	10.353	0.9579	0.9413	0.9527	28
13.90	10.591	0.9435	0.9252	0.9330	25
19.97	10.980	0.9241	0.8947	0.9034	22
26.06	11.527	0.9029	0.8428	0.8870	20

* f_o = Sinusoidal mode frequency at balanced operation [cf. equation (7.22)].

7.7.1 THE CIRCUIT AND THE ANALYSIS

The circuit using a matched pair of transistors (TD 101) and its partial equivalent for deriving the expression for the differential voltage in relation to the constant emitter current

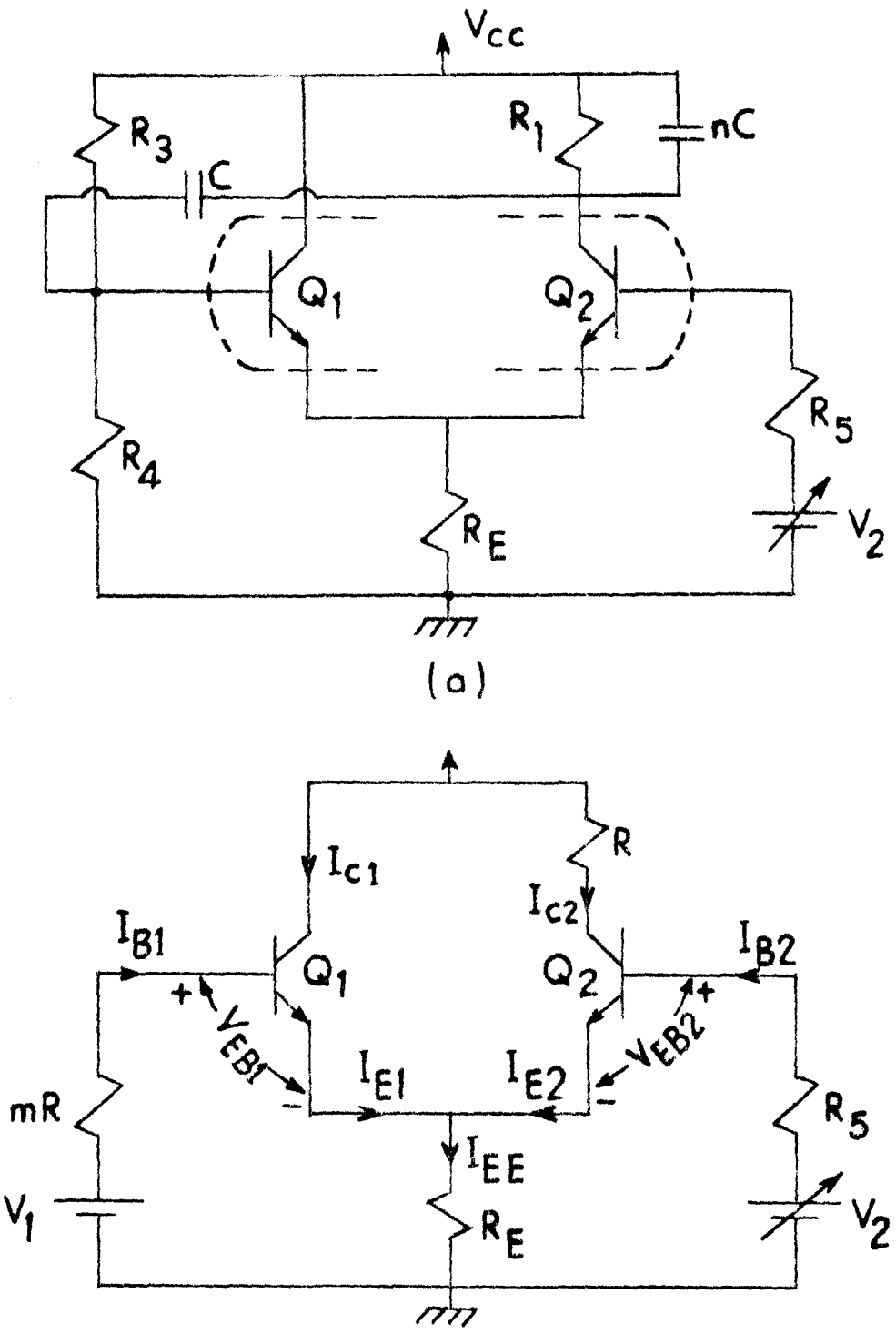

Fig.7.10 (a) VCO circuit

(b) Partial equivalent circuit of 7.10 (a)

and quiescent condition are shown in figures 7.10(a) and (b) respectively. The voltage source V_1 and resistance mR are the Thevenin generator and resistance as seen by the base of the transistor Q_1. The differential voltage is easily derived as (see appendix 7.1).

$$u = V_1 - V_2 + I_{c_2} \frac{mR + R5}{h_{fe}} - I_{EE} \frac{mR}{1 + h_{fe}} \qquad (7.20)$$

where h_{fe} is the common emitter current gain of the transistor.

From the logical development laid out above and from the transfer characteristics the desired relation is easily obtained as

$$g = ab = g_o \cosh^2 bu \qquad (7.21)$$

where g_o is the slope at the origin for balanced operation with given operating conditions. Combining equation (7.20) and (7.21), g can be obtained for different u, the corresponding ϵ and β are evaluated by using equation (7.6a) and (7.6b) and equation (7.7) is solved to obtain the frequencies. It should be remembered that every differential change in u produces a new asymmetric operating point with the changed value of g. Parameter g is obtained by considering average fixed value of b obtained from the balanced operating condition.

The asymmetric points may be obtained from the intersections of the graphs of equations (7.2) and (7.21). Presumably this shift in the operating points leads to distortion in waveform; however when the shift is kept small, sufficiently wide frequency variation

with low distortion is obtainable. With asymmetry thus limited the assumption of balanced operation shows good correlation between theoretical and experimental results as shown in Table-7.3.

Since operation is limited to the near harmonic mode, one is tempted to approximate equation (7.7) to classical van der Pol equation. In such cases one can have an approximate solution for frequency by using the method of small parameters[6], the frequency relation in which case is given by

$$f = f_o \left[1 - \frac{1}{16}\epsilon^2 + \ldots\right] \qquad (7.22)$$

where

$$f_o = \frac{1}{2\pi RC\sqrt{mn}}$$

The frequencies are calculated by using equation (7.7) for different values of u. Table-7.3 shows the results along with the measured distortion figures. For the variation of frequencies with respect to u given in Table-7.3 the distortion level is seen to be quite low. Further, it may be noted that the results are same, irrespective of the direction of change of u.

7.7.2 PRACTICAL SCHEME

As a practical utilization scheme to telemeter process data the variable voltage V_2 is replaced by a data-to-voltage source. The partial scheme is shown in figure 7.11. Test results have shown the same accuracy as obtained in Table-7.3.

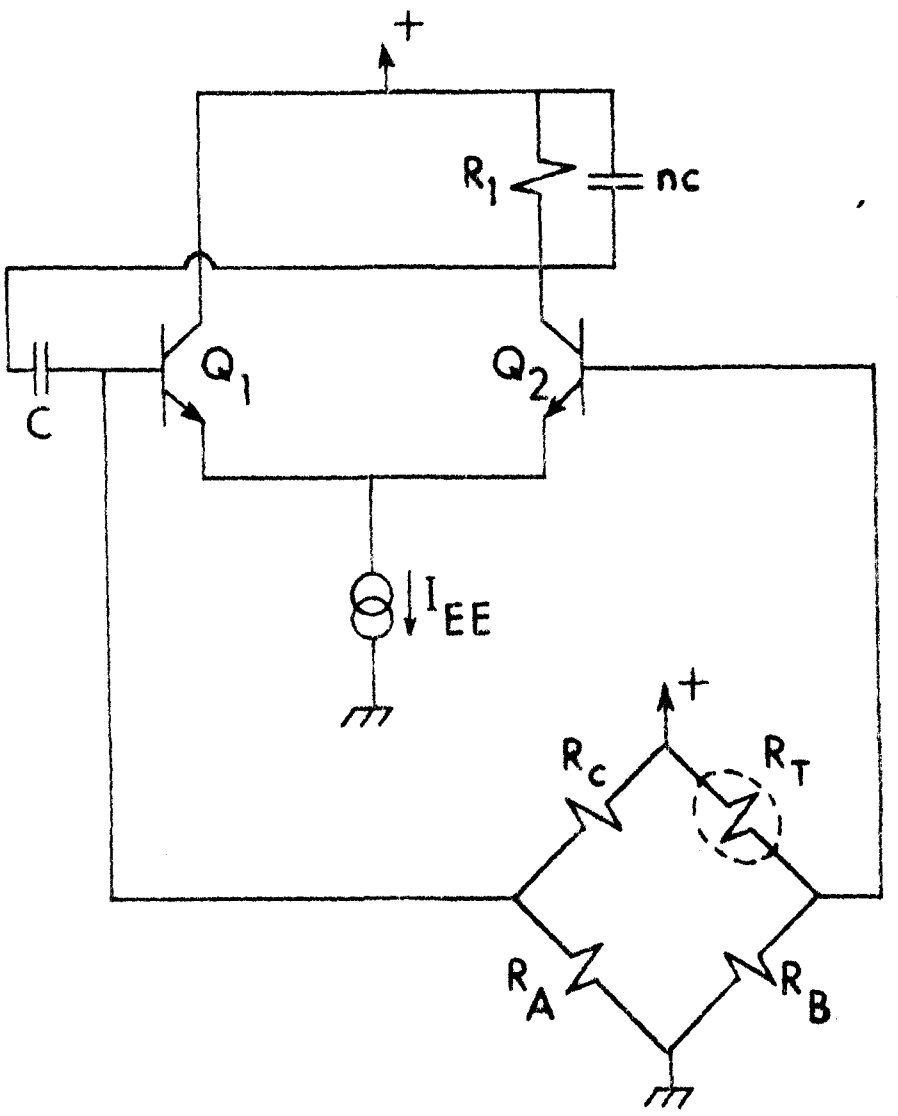

Fig.7.11. Scheme of a VCO using Resistance Thermometer for temperature telemetering $R_A = R_B$; $R_C = R_{Tn}$ is the resistance of the thermometer at reference temperature

7.7.3 DISCUSSIONS

Transistor base leakage currents have not been considered in deriving equation (7.20); this is quite justified for the silicon planar transistor used (TD 101). Results obtained with a pair of germanium transistors (2N483) show that, when leakage current is not negligible and the transistors have a low value of h_{fe}, a wider and a more linear frequency variation is obtainable for the same level of distortion with a larger variation of u. However, the analysis in this case becomes quite involved and as the leakage currents have to be accurately known, no attempt has been made to accommodate these in equation (7.20).

7.8 CONCLUSION

A nonlinear oscillatory system using the self-saturating antisymmetric transfer characteristic (ASTC) of an emitter coupled differential pair has been presented with a comprehensive analysis showing adjustability from sinusoidal to hard relaxation mode by two-parameter control, unlike the existing types of van der Pol oscillators where a single-parameter control is used. This approach completely explains the mode, frequency and waveform, and furnishes information as to selection ranges of the parameter values.

It should however be noticed that the two-parameter control can be effected by the variation of n_1 and n_2 the capacitor ratios, or ab the slope of the ASTC or by m the ratio of the resistors alone. Table-7.1 shows that even n_2 alone could change the mode from near sinusoidal to near relaxation oscillation. This implies the adaptability of such an oscillator to instrumentation system

with C_2 replaced by a capacitive transducer[7] to monitor a process variable. Differential capacitive transducer[7] could as well be used in place of C_1 and C and/or C_2 and C as each of the pair has a common terminal. The change in both frequency or amplitude could be a measure of the variable. The utility of this type of a generator is more as a waveform generator, as the change in waveform may not be quite acceptable for the signal processing purpose . Interestingly however if the operating slope ab is changed by changing the bias voltage of one of the transistors a wide frequency variation is obtained with very little waveform distortion and gives rise to a VCO with this differential pair. Such a VCO has also been studied and the results are given in Table-7.3. A partial practical scheme to replace the control bias source by a data-to-voltage source has also been shown indicating a practical utilization scheme of the VCO to telemeter process data and test results have shown the same accuracy as obtained in Table-7.3.

It is interesting to note that the hard relaxation mode only, can be analysed with an approximation that derives the frequency analytically within 5 to 10% tolerance and such an approximate analysis is discussed in the next chapter.

APPENDIX-7.1

From figure 7.10(b) the loop equations for loop 1 and loop 2 are

$$V_{EB1} + I_{EE}R_E - V_1 + I_{B1}\,mR = 0 \qquad \text{(A-7.1)}$$

$$V_{EB2} + I_{EE}R_E - V_2 + I_{B2}\,R_5 = 0 \qquad \text{(A-7.2)}$$

Subtracting equation (A-7.2) from equation (A-7.1) the differential base voltage u is obtained as

$$u = V_{EB1} - V_{EB2} = V_1 - V_2 + I_{B2}R_5 - I_{B1}mR \qquad \text{(A-7.3)}$$

The two transistors Q_1 and Q_2 being matched the common emitter current gain $\beta_1 = \beta_2 = \beta$, hence equation (A-7.3) is written as

$$u = V_1 - V_2 + \frac{1}{\beta}\,(I_{C2}R_5 - I_{C1}\,mR) \qquad \text{(A-7.3)}$$

For an emitter coupled differential transistor pair

$$I_{EE} = I_{E1} + I_{E2} \qquad \text{(A-7.4)}$$

or

$$I_{C1} = \alpha I_{EE} - I_{C2} \qquad \text{(A-7.5)}$$

where α is the common base current gain.

From equation (A-7.5) and equation (A-7.3)

$$u = V_1 - V_2 + \frac{1}{\beta}\left[I_{C2}\,(R_5 + mR) - \alpha I_{EE}\,mR\right]$$

$$= V_1 - V_2 + I_{C2}\,\frac{R_5 + mR}{h_{fe}} - I_{EE}\,\frac{mR}{1 + h_{fe}} \qquad \text{(A-7.6)}$$

where $\alpha = \dfrac{\beta}{\beta + 1}$ and $\beta = h_{fe}$.

REFERENCES

1. van der Pol,B. : 'The nonlinear theory of electric oscillation'; Proc. IRE, Vol.22, No.9, pp.1051-1082, Sept.1934.

2. Scott,P.R. : 'Large amplitude operation of the nonlinear oscillator'; Proc. IEEE, Vol.56, No.12, pp.2182-2183, December 1968.

3. Kundu,P. and Roy,S.B. : 'A temperature-stable RC transistor oscillator'; Proc. IEEE, Vol.57, No.3, pp.356-357, March 1969.

*4. Roy,S.B. and Patranabis,D. : 'Non-linear oscillations using antisymmetric transfer characteristics of a differential pair'; Int. J. Electron., Vol.42, No.1, pp.19-32, 1977.

*5. Roy,S.B. and Patranabis,D. : 'Voltage-controlled oscillator using an emitter-coupled differential pair'; Electron. Lett., Vol.13, No.19, pp.590-591, Sept. 1977.

6. Groszkowski,J. : 'Frequency of Self-Oscillations'; Oxford : Pergamon Press, 1964, pp.181-184.

7. Patranabis,D. : 'Principles of Industrial Instrumentation'; New Delhi : Tata McGraw-Hill, 1976, pp.60-62.

---

* Chapter-VII is based mainly on these two publications.